

## SOFT MAGNETIC NANOCRYSTALLINE Ni-Fe-X-Y AND $\text{MeFe}_2\text{O}_4$ POWDERS OBTAINED BY MECHANOSYNTHESIS

I. CHICINAȘ<sup>1\*</sup>, F. POPA<sup>1</sup>, B.V. NEAMȚU<sup>1</sup>, T.F. MARINCA<sup>1</sup>,  
O. ISNARD<sup>2</sup>, V. POP<sup>3</sup>

**ABSTRACT.** The soft magnetic nanocrystalline powders, alloys ( $\text{Ni}_3\text{Fe}$ , 79Ni16Fe5Mo, 77Ni14Fe5Cu4Mo, wt. %) and zinc ferrite, were obtained by dry and wet mechanical alloying and reactive milling, followed by different heat treatments. The powders were characterised by X-ray diffraction, scanning electron microscopy, X-ray microanalysis, differential scanning calorimetry, thermomagnetic and magnetic measurements. The X-ray diffraction shown the progressive new phases formation. The crystallite size is between 18-7 nm depending on materials and milling conditions. The particle size is smaller for wet-mechanical alloying comparing with dry-milling. The thermomagnetic measurement shown the Curie temperature of the alloys. The spontaneous magnetisation of the wet-milled and annealed samples is higher than of the molten alloys.

**Keywords:** mechanical alloying; Ni-Fe-X-Y alloys; soft ferrite; magnetisation; XRD; DSC.

### INTRODUCTION

Materials having crystallite/particle size smaller than 100 nm are known as nanocrystalline/nanostructured/nanosized materials. Nanocrystalline materials have unique properties if their crystallites are smaller than the characteristic length of the physical phenomena occurring in bulk materials. These different properties derive from the large number of atoms placed at the grain boundaries, interfaces/

---

<sup>1</sup> Materials Science and Engineering Department, Technical University of Cluj-Napoca, 103-105 Muncii Ave., 400641 Cluj-Napoca, Romania

<sup>2</sup> Institut Néel, CNRS / Université Grenoble Alpes, 25 rue des Martyrs, BP166, 38042 Grenoble, Cédex 9, France

<sup>3</sup> Babeș-Bolyai University, Faculty of Physics, 1 Kogălniceanu Str., 400084 Cluj-Napoca, Romania

\* Corresponding author: ionel.chicinas@stm.utcluj.ro

interphases as compared to the same materials in the polycrystalline state [1-3]. Thus, the atoms located at interfaces determine decisively the physical/mechanical properties of the nanocrystalline materials. The benefits of the nanocrystalline state are due to chemical and structural variations on a nanoscale, very important to having optimal magnetic properties [1,2,4]. The very low coercivity in the nanocrystalline materials is different from superparamagnetic behaviour, where low coercivity come together with a low permeability. Due to the coupling of small ferromagnetic crystallites by exchange interactions, the nanocrystalline materials have simultaneously low coercivity and high permeability [5]. Such behaviour was explained by the random anisotropy model [6].

Fe–Ni alloys around the Ni<sub>3</sub>Fe (Permalloy) composition and Fe–Ni–(X–Y) alloys, known as Supermalloy, are widely used for their high properties as soft magnetic materials. The production of these materials as nanocrystalline powders can add interesting properties. The interesting properties (superparamagnetic state, spin canting effect, partial redistribution of the cations) can be obtained in the nanocrystalline/nanosized ferrites prepared by mechanical activation and mechanosynthesis, which were reviewed in Ref. [7].

In last decades, the different mechanosynthesis routes used in developing soft magnetic nanocrystalline powders (ferrites and alloys) or nanocomposite powders were reported. Here we summarize our contributions on obtaining new materials by mechanosynthesis with an emphasis on the Ni-Fe-(X-Y) and ferrites soft magnetic nanocrystalline powders obtained by mechanical alloying and reactive milling. Some results have been previously reported [8-25].

## **MATERIALS AND METHODS**

For Ni-Fe and Ni-Fe-X-Y alloys producing the following elemental powders were used as starting materials: 123-carbonyl nickel, NC 100.24 (Höganäs) iron, Mo powder produced by chemical reduction and copper powder. The powder mixtures with the following composition were used: Ni<sub>3</sub>Fe, 79Ni16Fe5Mo (wt. %) and 77Ni14Fe5Cu4Mo (wt. %). The soft magnetic ferrites were obtained from equimolar mixture of high purity commercial oxide powders (Alpha Aesar), MeO (Me = Ni, Cu, Zn) and iron oxide ( $\alpha$ -Fe<sub>2</sub>O<sub>3</sub>—haematite).

All the mixtures of elemental powders or oxides, before milling, were homogenised for 15 minutes using a Turbula type apparatus. For mechanical alloying the starting mixtures (“ss” sample) were dry or wet milled in argon atmosphere using a planetary ball mill (Fritsch, Pulverisette 4 and Pulverisette 6). For wet milling

2 ml of benzene was added after each vial opening (for sampling) in order to avoid powders agglomeration via cold welding. The milling process were carried out in stainless steel vials (with 500 cm<sup>3</sup> volume), using stainless steel balls with 15 mm diameter. The ball to powder mass ratio (BPR) was between 8:1 and 10:1. Several milling times were used ranging from 1 to 12-28 hours, depending on mill and alloy. The milled powders were annealed in vacuum at 350 °C and 400 °C during 0.5 to 4 h to remove the internal stresses and also to finish the solid-state reaction leading to synthesis of a new phase. The nanocrystalline soft ferrites were obtained by reactive milling in air, using the same mill equipment. The ball to powder mass ratio (BPR) was 15:1.

The evolution of formation of new phases (alloy or ferrite) by milling was investigated by X-ray diffraction (XRD) in the angular range  $2\theta = 25\text{--}100^\circ$  using a Siemens D5000 diffractometer, operating with  $\text{CoK}\alpha$  radiation ( $\lambda = 1.7903 \text{ \AA}$ ) and Bruker D8 diffractometer operating with  $\text{CuK}\alpha$  radiation ( $\lambda = 1.5418 \text{ \AA}$ ). The mean crystallite size was determined on the milled and annealed samples from full-width-at-half maximum (FWHM) of the diffraction peaks using Scherrer's formula [26] and by Williamson-Hall method, on the as-milled samples [27].

Thermal stability of the samples was studied by a Setaram Labsys differential scanning calorimetry (DSC) apparatus, using high purity alumina as reference in the 25 – 800 °C temperature range using argon atmosphere. The heating/cooling rate was 10 °C/min.

The powders morphology and the local chemical homogeneity of the particles were investigated by scanning electron microscope (SEM, Jeol-JSM 5600 LV) equipped with an energy dispersive X-ray spectrometer (EDX, Oxford Instruments, Inca 200 soft).

The magnetisation measurements ( $M(H)$ ) were made by the extraction sample method at 300 K and a maximum magnetic field of 8 T. The Curie temperatures of different phases were determined by thermomagnetic measurements.

## RESULTS AND DISCUSSIONS

The XRD patterns for the powders obtained by mechanical alloying (MA) for times ranging from 2 to 28 h show a progressive formation of  $\text{Ni}_3\text{Fe}$  intermetallic compound by MA (Fig. 1). The iron Bragg peaks are vanished and after 6 hours of milling, they are indistinguishable from the background noise. This fact suggests the idea that iron atoms either formed a compound with nickel ( $\text{Ni}_3\text{Fe}$ ), or formed a Ni-Fe solid solution. At the same time, a shift of the peaks towards the small angles is

observed. The shift to small angles is due (i) to the formation of the  $\text{Ni}_3\text{Fe}$  intermetallic compound and (ii) to the first order stresses induced by milling. The new peak positions after 10 hours of milling are at smaller angles than the  $\text{Ni}_3\text{Fe}$  positions, as a consequence of the first order internal stresses.

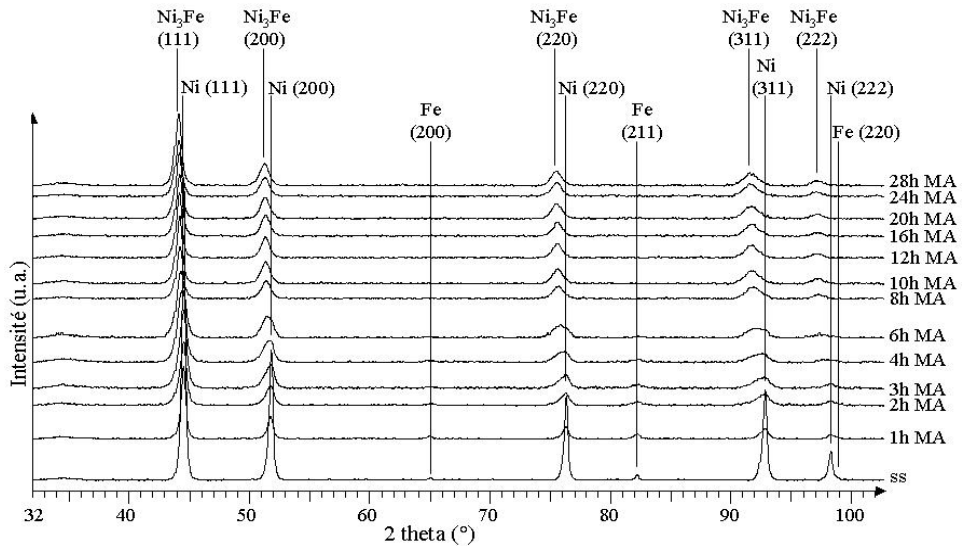


**Fig. 1.** X-ray diffraction patterns ( $\text{Cu K}\alpha 1$ ,  $\lambda = 1.5406 \text{ \AA}$ ) for samples milled up to 28 hours. ss refers to the starting sample. For clarity, the spectra have been shifted vertically. There are indicated the positions of the Bragg peaks of nickel, iron and  $\text{Ni}_3\text{Fe}$ .

The influence of the annealing conditions (temperature and time) on the  $\text{Ni}_3\text{Fe}$  formation is shown for 8 h milled sample, figure 2. For 8 h as-milled sample a broad diffraction peak is observed at the  $\text{Ni}_3\text{Fe}$  position, accompanied by another peak of lower intensity which corresponds to the unreacted nickel during milling. After only 30 minutes of annealing at  $400 \text{ }^\circ\text{C}$ , the intensity of the  $\text{Ni}_3\text{Fe}$  maxima increases and the Ni maxima has disappeared. By increasing the annealing time, the intensity of the  $\text{Ni}_3\text{Fe}$  maximum increases and also the maximum shifts towards large angles as a consequence of the internal stresses' removal. After 4 hours of annealing the peak position is at the same position as for  $\text{Ni}_3\text{Fe}$  obtained by fusion, as an effect of the stresses removal and finishing the solid-state reaction [28].

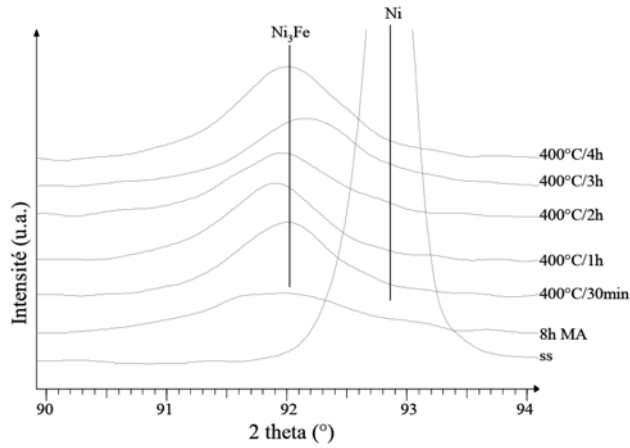


**Fig. 2.** The influence of annealing conditions on the (311)  $\text{Ni}_3\text{Fe}$  maxima of the samples milled 8 hours. ss denote the starting mixture.

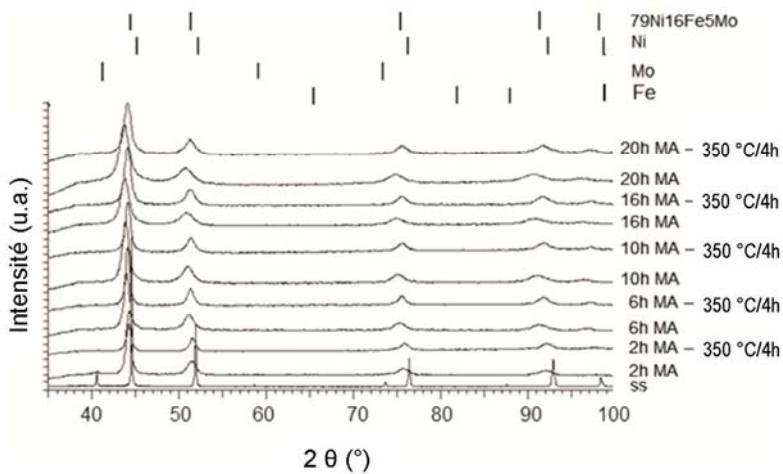


**Fig. 3.** X-ray diffraction patterns of 79Ni16Fe5Mo (wt %) mechanically wet-milled powders up to 20 hours and mechanically wet-milled and followed by annealing at 350°C for 4 hours ( $\lambda_1 = 1.5406 \text{ \AA}$ ). To clarify the diffractograms were vertically shifted. The starting mixture was indicated by the acronym ss. [29].

The evolution of the Superalloy 79Ni16Fe5Mo (wt. %) formation by wet-milling up to 20 hours and annealing (350 °C for 4 h) is shown in figure 3. It can be shown a movement towards smaller angles and a broadening of the Bragg peaks by increasing the milling time. This displacement of the Bragg peaks is caused, similar

to Ni<sub>3</sub>Fe alloy, by the formation of the alloy and by the first-order internal stresses that are induced by milling. X-ray patterns of the annealed samples show a better definition of diffraction peaks. The X-ray diffraction patterns of 79Ni16Fe5Mo powder after 6 hours of wet-milling followed by annealing shows that Bragg maxima correspond those of the alloy of the same composition obtained by fusion [29].

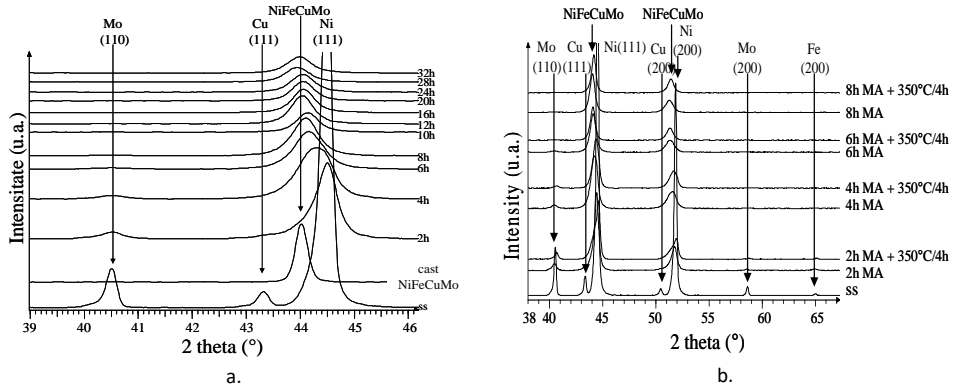


**Fig. 4.** X-ray diffraction patterns of 77Ni14Fe5Cu4Mo (wt. %). a - mechanically dry-milled powders up to 32 hours; b - mechanically dry-milled and followed by annealing at 350°C for 4 hours ( $\lambda = 1.5406 \text{ \AA}$ ). To clarify the diffractograms were vertically shifted. The starting mixture was indicated by the acronym ss.

The evolution of the Mümetal (77Ni14Fe5Cu4Mo, wt. %) formation by milling up to 32 hours and annealing (350°C/4 h) is shown in figure 4 a, b. A displacement towards smaller angles and a broadening of the Bragg peaks by increasing the milling time was observed. In figure 4a, in the case of as-milled powders, the Cu, Fe and Mo Bragg peaks disappear after 4, 6 and 10 hours of milling respectively. By annealing the Mümetal alloy is formed after 8 hours of milling followed by an annealing at 350 °C/4 hours, figure 4b [28].

The evolution of Zn ferrite obtaining by reactive milling (RM) is shown in figure 5. After 4 hours of milling, they are noticed new, intense maxima, that correspond to the newly formed phase, zinc ferrite. Simultaneously with the appearance of these maxima also shows the disappearance of the maxima characteristic of zinc oxide, which indicates a rapid and complete amorphization of it or a diffusion of Zn and O atoms in the structure of iron oxide [30, 31]. Iron oxide maxima are much flattened (those that are visible in the diffractogram), but most can no longer be identified in diffractogram. The corresponding maxima of ZnFe<sub>2</sub>O<sub>4</sub> are much more intense compared to the maximum of the unreacted iron oxide, which suggests that at this time of milling (4 hours) the major phase is Zn ferrite. The presence of elemental iron in the sample is

due to contamination of the powder on during milling. [31, 32]. Prolonged milling time (20-30 h) lead to a reaction between zinc ferrite and iron provided by contamination resulting in a wüstite type phase. The as-milled samples were subjected to a heat treatment in vacuum and in air at temperatures of 400, 500, 600, 700 and 800 °C for 4 hours. At temperatures higher than 500 °C a decomposition of the Zn ferrite with the presence of  $\text{Fe}_2\text{O}_3$  was evidenced. The heat treatment at 500 °C for 4 hours in the air is the only one we have a complete ferrite formation for all milling times. More information of  $\text{ZnFe}_2\text{O}_4$ ,  $\text{NiFe}_2\text{O}_4$ ,  $\text{CuFe}_2\text{O}_4$  can be found in Ref [30]. All milled samples (alloys and ferrites) obtained by MA and RM are in the nanocrystalline state. The crystallite size of the Ni-Fe alloys decreases by increasing milling time, up to 18 – 7 nm, depending on alloys, milling equipment or type o milling (wet or dry) [28, 29]. The crystallite size of  $\text{ZnFe}_2\text{O}_4$  powders obtained by RM is of  $8 \pm 2$  nm after 30 hours of milling [30].

In Figure 6 are presented the SEM images of 77Ni14Fe5Cu4Mo powders

Wet milled for 4, 8 and 20 hours. The decrease of particle size with increasing milling time can be observed. In addition, for longer milling times (8 hours), particles with rounded corners can be observed. The two causes that lead to the decrease the size of the particles are, on the one hand, the stresses induced in the material by the milling, which reduce the plasticity of the material and, on the other hand, the presence of benzene on the surface particles that prevents cold welding processes. The same powders morphology evolution can be found for all samples obtained by MA.

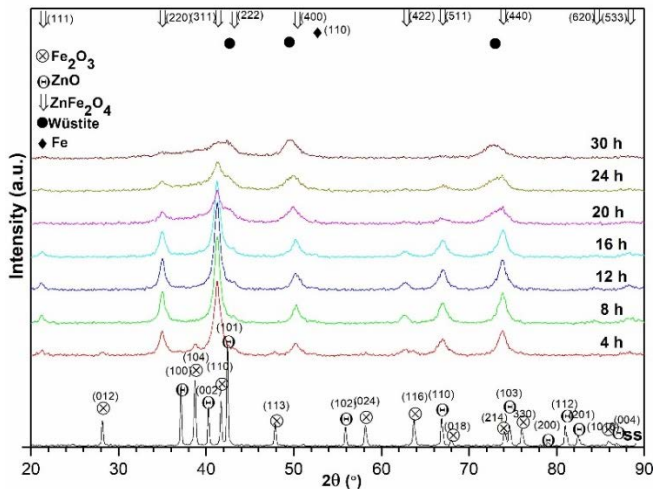


**Fig. 5.** XRD patterns of the as-milled samples (4, 8, 12, 16, 20, 24 and 30 h). The starting sample is noted by ss. For clarity, the spectra have been shifted vertically. The XRD maxima for different phases are marked.

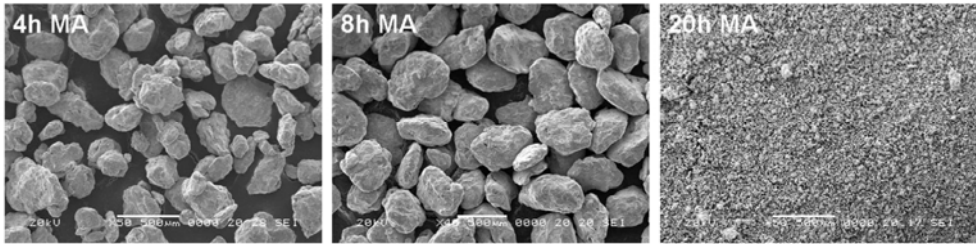


**Fig. 6.** SEM images of 77Ni14Fe5Cu4Mo powder milled for 4, 8 and 20 hours at magnification of 50x.

The DSC curves of the milled samples were evidenced the phase transformations in the powders during heating and cooling, such as: internal stresses removal, recrystallisation, Curie temperature and their changes with milling conditions. An interesting behaviour was observed on the DSC curves of the wet-milled samples, where the presence of an exothermic peak for all wet-milled samples can be observed, figure 7. This peak was attributed to the elimination of benzene adsorbed on the surface of powders. The elimination of benzene results from the thermal activation and the catalytic behaviour of Ni, Fe and Mo on the decomposition of benzene [33, 34]. concerning the exothermic peaks presented in figure 6 one can observe that (i) their surface increases (by a factor of 4), and (ii) a shift towards lower temperatures when the milling time increases (from 495 °C to 431 °C for a milling time of 4 and 20 hours respectively). The increase in the surface of the DSC peaks is related to the increase of the amount of benzene adsorbed on the surface and inside particles. A complete analysis of the presence of this exothermic peak in Ni<sub>3</sub>Fe powders wet-milled was presented in Ref. [35].

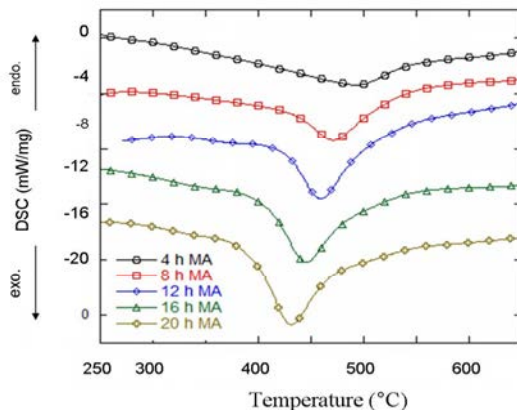


**Fig. 7.** DSC heating curves for 77Ni14Fe5Cu4Mo samples, wet-milled in benzene for 4, 8, 12, 16 and 20 hours. For more than clarity, the DSC curves have been shifted vertically. The atmosphere used in DSC was Ar + 5% H<sub>2</sub>



Thermomagnetic analysis offers the advantage of in-situ alloying study during heat treatment. Thermomagnetic measurements in a low field (less than 0.1 T) are shown in figure 8. These measures show the progressive formation of the alloy by MA, and by milling followed by annealing. For the starting sample (ss), the  $M^2$  curve versus temperature shows two transitions on heating: one at the Curie temperature of nickel ( $T_C = 631$  K) and the other at the Curie temperature of iron ( $T_C = 1043$  K). On cooling, the  $M^2(T)$  curve shows a mixture of ferromagnetic phases with the Curie temperatures over a wide range. These phases were formed at high temperature by the local diffusion of nickel, molybdenum and copper small particles in the larger iron particles. This can be explained by the fact that in the starting mixture there are large iron particles (average particle size is  $< 40 \mu\text{m}$ ), surrounded by much smaller particles of nickel and molybdenum (about  $5 - 7 \mu\text{m}$ ). For the sample milled 4 h, on the heating curve is observed the Curie temperature of unreacted Ni and also the Curie temperature of the NiFeCuMo alloy formed by MA (a small change in the slope curve). Also, a progressive alloying process by heating with formation of a mixture of phases can be observed. No transition at the Curie temperature of iron is detected, because iron reacted with the other elements under the influence of temperature before 1043 K. By heating up to 1100 K, the  $77\text{Ni}14\text{Fe}5\text{Cu}4\text{Mo}$  alloy is formed in the whole sample volume and, consequently, on the cooling curve only one Curie temperature is observed. The process is the same for the 10 h milled sample, but the amount of the unreacted elements during milling is very little. For 16 h milled sample, on the heating curve a single transition is visible at a temperature of 630 K (the Curie temperature of the alloy), but at cooling the transition is shifted towards higher temperatures. The difference between the Curie temperatures at heating and at cooling could be due to the appearance of an iron-rich phase. This can be due to the powder contamination with iron during milling at high milling time and under the influence of very high temperature iron-rich phases can form (the  $\text{Ni}_3\text{Fe}$  maybe). A complete analysis of the thermomagnetic measurements on the synthesis of nanocrystalline Supermalloy powders by mechanical alloying is presented in Ref. [17].

The spontaneous magnetization of the samples milled for 8 and 12 hours before and after annealing at  $350 \text{ }^\circ\text{C}/4$  hours is shown in figure 9. It is notable that the annealing leads to an increase of the value of the powder's spontaneous magnetization. This fact can be explained by the elimination of internal stresses and the decrease in the density of crystalline defects induced during milling. By comparing the value of the spontaneous magnetization of the annealed samples with the spontaneous magnetization of the molten alloy, also shown in the figure 9, it is obvious that the magnetizations for samples obtained by wet-milling are slightly higher. This

can be due to the contamination with iron from the balls and vials used, contamination that was observed during EDX analyses. It is well known that in the dry milling a protective layer from the materials milled is formed on the surface of the balls and vials which prevents or decreases the powder contamination. In the case of wet-milling, this protection layer is absent or too thin and its thickness may not be sufficient to prevent powder contamination.

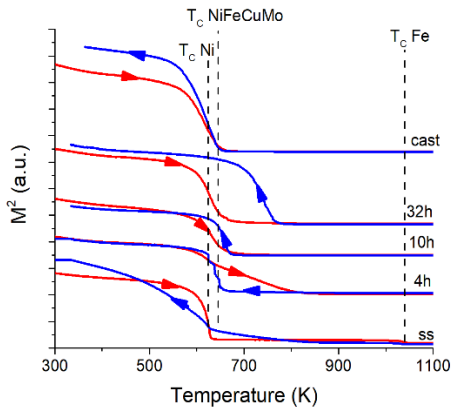


**Fig. 8.** The magnetization versus temperature for 77Ni14Fe5Cu4Mo powders milled 4, 10 and 32 hours. The starting sample (ss) and the cast sample are also presented.

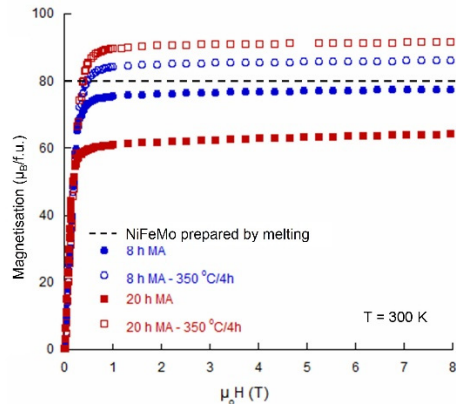


**Fig. 9.** Influence of annealing at 350 °C/4 hours on the magnetization value of Supermalloy (79Ni16Fe5Mo, wt. %) powders wet-milled for 8 and 20 hours.

## CONCLUSIONS

The mechanosynthesis route is a powerful tool for producing soft magnetic nanocrystalline materials, both alloys and ceramic compounds. A large variety of Ni-Fe alloy have been successfully produced by mechanical alloying in nanocrystalline state. Also, by reactive milling Cu, Zn and Ni ferrites with cubic spinel structure have been produced effectively. In both cases the structure is formed progressively upon increasing the milling time. The alloying time needed for fully obtaining the desired phase is depending on the processed materials. For both, alloys and ferrites a contamination of the powders with iron provided by vials and ball for prolonged milling times was noticed. The crystallites size is in nanometric range when the alloy/compound starting to form. The annealing, in general, improve the magnetic characteristic of the as-milled samples. The structural and magnetic characteristics are strongly dependent on the synthesis conditions. The magnetic measurements

show a decrease of the magnetisation upon milling process, with a strong restauration after annealing. The thermomagnetic measurement is a strong instrument in observation of the alloys formation and theirs iron contamination for large milling times.

## REFERENCES

- [1] C. Suryanarayana, *Int. Mater. Reviews*, 40, 41 (1995).
- [2] K. Lu, *Mater. Sci. Eng.*, R16, 161 (1996).
- [3] S.C. Tjong, H. Chen, *Mater. Sci. Eng.*, R41, 1 (2004).
- [5] G. Herzer, Nanocrystalline Soft Magnetic Alloys, in Handbook of Magnetic Materials, Ed. by K.H.J. Buschow, Elsevier Science BV (1997).
- [6] G. Herzer, *Physica Scripta*, T49, 307 (1993).
- [7] V. Šepelák, I. Bergmann, S. Kips, K.D. Becker, *Z. Anorg. Allg. Chem.*, 631, 993 (2005).
- [8] I. Chicinaş, V. Pop, O. Isnard, *J. Magn. Magn. Mater.*, 242-245, 885 (2002).
- [9] I. Chicinaş, V. Pop, O. Isnard, J.M. Le Breton, J. Juraszek, *J. Alloys Compd.*, 352, 34 (2003).
- [10] V. Pop, O. Isnard, I. Chicinaş, *J. Alloys Compd.*, 361, 144 (2003).
- [11] I. Chicinaş, V. Pop, O. Isnard, *J. Mater. Sci.*, 39, 5305 (2004).
- [12] O. Isnard, V. Pop, I. Chicinaş, *J. Magn. Magn. Mater.*, 290-291, 1535 (2005)
- [13] Z. Sparchez, I. Chicinaş, O. Isnard, V. Pop, F. Popa, *J. Alloys Compd.*, 434-435, 485 (2007).
- [14] F. Popa, O. Isnard, I. Chicinaş, V. Pop, *J. Magn. Magn. Mater.*, 316, e900 (2007).
- [15] V. Pop, I. Chicinaş, *J. Optoelectron. Adv. Mater.*, 9, 1478 (2007).
- [16] B.V. Neamtu, O. Isnard, I. Chicinaş, V. Pop, *IEEE Trans. Magn.*, 46, 424 (2010).
- [17] F. Popa, O. Isnard, I. Chicinaş, V. Pop, *J. Magn. Magn. Mater.*, 322, 1548 (2010).
- [18] B.V. Neamtu, I. Chicinaş, O. Isnard, F. Popa, V. Pop, *Intermetallics*, 19, 19 (2011).
- [19] T.F. Marinca, I. Chicinaş, O. Isnard, V. Pop, *Optoelectron. Adv. Mater. - Rapid Commun.*, 5, 39 (2011).
- [20] B.V. Neamtu, O. Isnard, I. Chicinaş, V. Pop, *J. Alloys Compd.*, 509, 3632 (2011).
- [21] T.F. Marinca, I. Chicinaş, O. Isnard, V. Pop, F. Popa, *J. Alloys Compd.*, 509, 931 (2011).
- [22] F. Popa, I. Chicinaş, O. Isnard, V. Pop, *J. Therm. Anal. Calorim.*, 110, 295 (2012).
- [23] F. Popa, O. Isnard, I. Chicinaş, V. Pop, *J. Alloys Compd.*, 554, 39 (2013).
- [24] I. Chicinaş, T.F. Marinca, B.V. Neamtu, F. Popa, O. Isnard, V. Pop, *IEEE Trans. Magn.*, 50, Article Number: 2800704 (2014).
- [25] I. Chicinaş, T.F. Marinca, B.V. Neamtu, P. Pascuta, V. Pop, *J. Therm. Anal. Calorim.*, 118, 1269 (2014).
- [26] P. Scherrer, *Nachr Gött Mathematisch Phys Klasse I*, 98 (1918).
- [27] G.K. Williamson, W.H. Hall, *Acta Metall.*, 1, 22 (1953).
- [28] F. Popa, Ph. D. Thesis, Technical University of Cluj-Napoca and Joseph Fourier University, Grenoble, 2008.

- [29] B.V. Neamtu, Ph. D. Thesis, Technical University of Cluj-Napoca and Joseph Fourier University, Grenoble, 2010.
- [30] T.F. Marinca, Ph. D. Thesis, Technical University of Cluj-Napoca, 2011.
- [31] T. F. Marinca, I. Chicinaș, V. C. Prică, F. Popa and B. V. Neamțu, *Mater. Sci. Forum*, 672, 149 (2011).
- [32] T. Verdier, V. Nachbaur, J. Malick, *J. Solid State Chem.*, 178, 3243 (2005).
- [33] J. E. Zanetti and G. Egloff, *J. Ind. Eng. Chem.*, 9, 350 (1917).
- [34] S. Ahmed, A. Aitani, F. Rahman, A. Al-Dawood, F. Al-Muhaish, *Appl. Catalysis A*, 359, 1 (2009).
- [35] B.V. Neamțu, O. Isnard, I. Chicinaș, C. Vagner, N. Jumate, P. Plaindoux, *Mater. Chem. Phys.*, 125, 364 (2011).